



# Laminar Burning Velocity and Cellular Instability of Iso-Octane/N-Butanol–Air Premixed Flames

Shanshan Chen<sup>1,2\*</sup><sup>1</sup> Department of Environmental Science, Hebei University of Environmental Engineering, 066102 Qinhuangdao, China<sup>2</sup> State Key Laboratory of Fire Science, University of Science and Technology of China, 230026 Hefei, China

\* Correspondence: Shanshan Chen (chenshanshan@hebuee.edu.cn)

**Received:** 04-20-2025**Revised:** 06-03-2025**Accepted:** 06-15-2025**Citation:** S. S. Chen, “Laminar burning velocity and cellular instability of iso-octane/n-butanol–air premixed flames,” *Power Eng. Eng. Thermophys.*, vol. 4, no. 2, pp. 121–130, 2025. <https://doi.org/10.56578/peet040204>.

© 2025 by the author(s). Licensee Acadlore Publishing Services Limited, Hong Kong. This article can be downloaded for free, and reused and quoted with a citation of the original published version, under the CC BY 4.0 license.

**Abstract:** The combustion behavior of blended petroleum–biofuel mixtures has increasingly been investigated as interest grows in low-toxicity, biodegradable, and energy-dense biomass-derived fuels. Among higher alkanols, n-butanol is recognized for its favorable physicochemical properties and its compatibility with gasoline-range hydrocarbons (HC) such as iso-octane. In this context, a systematic evaluation of laminar flame propagation and instability characteristics is essential for understanding the combustion performance and operational safety of blended fuels. In the present study, the laminar burning velocity (LBV) and cellular instability of premixed iso-octane/n-butanol/air flames were quantified for a wide range of equivalence ratios (0.7–1.5) at an initial temperature of 423 K and ambient pressure. It was observed that the LBV increased consistently with the addition of n-butanol, whereas the Markstein length ( $L_b$ ) decreased. Analysis of cellular structures revealed that diffusive-thermal instability strengthened monotonically as the equivalence ratio increased, resulting in more unstable flame propagation under fuel-rich conditions. In contrast, the hydrodynamic instability exhibited a non-monotonic trend, first intensifying and subsequently diminishing with increasing equivalence ratio. The critical Peclet number decreased continuously across the equivalence-ratio range, while the critical flame radius varied non-monotonically. The incorporation of n-butanol was found to enhance both diffusive-thermal and hydrodynamic instabilities and to reduce the critical Peclet number and critical flame radius. These findings underscore the need for careful control of combustion stability in practical applications involving iso-octane/n-butanol mixtures and provide fundamental insight into the flame-structure evolution associated with next-generation alternative fuels.

**Keywords:** Laminar burning velocity; Flame stability; Iso-octane; N-butanol

## 1 Introduction

Currently, 80% of the world’s energy demand is met by fossil fuels such as coal, oil, and natural gas. However, the environmental problems caused by fossil fuel combustion, rising prices, and the depletion of natural energy sources like oil reserves have encouraged researchers to seek alternative energy sources that are cost-effective, sustainable, renewable, and efficient [1, 2]. According to a report by the U.S. Energy Information Administration, global energy consumption will increase by 71% between 2000 and 2030, and carbon dioxide (CO<sub>2</sub>) emissions are expected to rise by approximately 35% during the same period. To limit the use of fossil fuels and reduce the greenhouse gases released by their combustion, the exploration of renewable energy sources has attracted growing attention. The proposal of the “dual carbon” goals (carbon peaking and carbon neutrality) indicates that China’s energy system is in urgent need of establishing a new pattern of low-carbon development. The fundamental path to carbon neutrality lies in the orderly phasing-out of fossil energy, and renewable fuels are regarded as the optimal alternative. On June 1, 2022, the “14<sup>th</sup> Five-Year Plan for Development of Renewable Energy” was jointly issued by the National Development and Reform Commission, the National Energy Administration, and other relevant departments, which requires steadily advancing the diversified development of biomass energy and vigorously developing non-grain biomass liquid fuels.

Biomass fuels, derived from biological products and matching the performance of petroleum and diesel, are known as biodiesel [3]. Compared with fossil fuels, biomass fuels can protect the environment by reducing the

emissions of greenhouse gases such as CO<sub>2</sub>, carbon monoxide (CO), sulfur dioxide (SO<sub>2</sub>), and hydrocarbons (HC). Therefore, they are regarded as clean energy and have attracted attention in the global fuel market owing to their low toxicity and high biodegradability, aiming to address issues like the energy crisis and environmental pollution. The components of biomass fuels belong to the alkanol category, among which methanol, ethanol, and butanol are the most representative in sequence [4]. Ethanol has advantages such as high octane value and high vaporization heat, and is commonly mixed with gasoline for use in many countries. It holds the largest market share which is growing rapidly. Compared with ethanol, butanol is considered to have a higher energy content and can allow for a longer driving range. Despite the growing interest in alternative fuels, achieving the goal of carbon neutrality still requires comprehensive planning and orderly advancement. Currently, petroleum fuels remain dominant, and biomass fuels are usually blended with traditional petroleum-based fuels in practical applications. Petroleum fuels are complex mixtures of different types of HC, including normal alkanes, isoparaffins, alkenes, cycloalkanes, and aromatics. To improve sustainable gasoline combustion technology in the face of economic, technological, and social challenges, it is necessary to thoroughly understand the physical and chemical kinetic properties of blended fuels.

As one of the key parameters describing the propagation characteristics of laminar premixed flames, the LBV integrates information on chemical reactions, mass diffusion, and heat release. It serves as a characteristic parameter for describing turbulent flame structures and can be used as an important input for turbulent combustion modeling. The unstretched LBV is an intrinsic property, which is only related to the composition and initial state of the premixed combustible gas. Gülder [5] conducted research on the mixtures of iso-octane and ethanol for the first time. Since then, researchers have typically studied such mixtures using the combustion bomb flame method or the heat flux method. To better understand the combustion speed of alternative fuels, Van Lipzig et al. [6] carried out studies on the mixtures of n-heptane and ethanol, as well as the mixtures of iso-octane, n-heptane and ethanol, and established empirical mixing rules for the LBV of gasoline-ethanol blended fuels. Dirrenberger et al. [7] were the first to measure the burning velocities of commercial gasoline and its alternative mixtures (including n-heptane, iso-octane, toluene and ethanol mixed) using the heat flux method. Manna et al. [8] investigated different but similar gasoline alternative fuels in spherical flames, formulated by blending toluene and ethanol. Meng et al. [9] determined the combustion speed of the surrogate fuels where the contents of iso-octane, toluene and 1-hexene were each 1/3 and were mixed with ethanol in different proportions.

Cellular instability is an inherent characteristic of laminar premixed flames. Under the influence of instability and disturbances, a certain number of cracks and wrinkles form on the flame front. As the flame propagates, these wrinkles and cracks continue to split and become denser, presenting cell morphology with different structures. The cellular structures on the flame front split at an accelerated rate with the expansion of the flame, eventually reaching a state of complete instability and even developing into a self-turbulization phenomenon [10]. Cellular instability and the critical state of instability serve as a transition from laminar flow to turbulence. In-depth research on the laws governing fuel flame instability and its critical state holds strong theoretical significance for studying fire phenomena such as turbulence and deflagration, which can provide practical data support for the safe development of alternative fuels as well. An explicit expression for the critical flame size was proposed by Bechtold and Matalon [11] with respect to physicochemical parameters in a spherically expanding flame. Addabbo et al. [12] conducted a theoretical investigation on the onset of the instability and subsequent development of cells on spherically expanding flames. Studies have been carried out to investigate the cellular instabilities of various combustible mixtures, including hydrocarbon-air and oxygenated fuel-air flames [13–15].

The objectives of this study focus on the LBV and cellular instability of premixed iso-octane/n-butanol-air flames. Flames with various mixing ratios at different equivalence ratios were predicted at an initial temperature of 423 K and pressure of 1 atm. The unstretched LBV was first investigated. Then the analysis of Markstein length ( $L_b$ ) was conducted to characterize the sensitivity of flame propagation to local stretch. Finally, the cellular instability was discussed and stated through two significant instabilities, namely the diffusive-thermal instability and hydrodynamic instability, and the critical condition at which the flame status turns stable into unstable was also evaluated.

## 2 Numerical Method

### 2.1 Kinetic Modeling

The detailed chemical kinetic models proposed by Ranzi et al. [16] and Li et al. [17] were employed in this study. The Ranzi Kinetic Model was constructed for the pyrolysis and combustion of a large variety of fuels at high-temperature conditions. This sophisticated mechanism contains 249 species and 8153 reactions and its comprehensive nature has been emphasized by researchers. The Li Kinetic Model of n-butanol/iso-octane blends comprises 133 species and 923 reactions, which has been validated against laminar flame speeds and ignition delay times, and proved to be applicable and reliable. Numerical simulations were carried out using the premixed laminar flame speed model in Chemkin-Pro software, with mixture-averaged transport and the Soret effect adopted.

Before setting the grid parameters to obtain the final solution, grid independence verification was first conducted. As shown in Figure 1, when the number of grid points increases from 760 to 1590, the difference in the laminar

flame propagation speed is 0.29 cm/s by 0.53%, which can be almost negligible. Obviously, when the number of grid points is sufficiently large, the laminar flame propagation speed obtained from the simulation remains almost constant. Therefore, it can be considered that the final number of grid points which ranged approximately 700 in this study is adequate to ensure a fully converged solution.

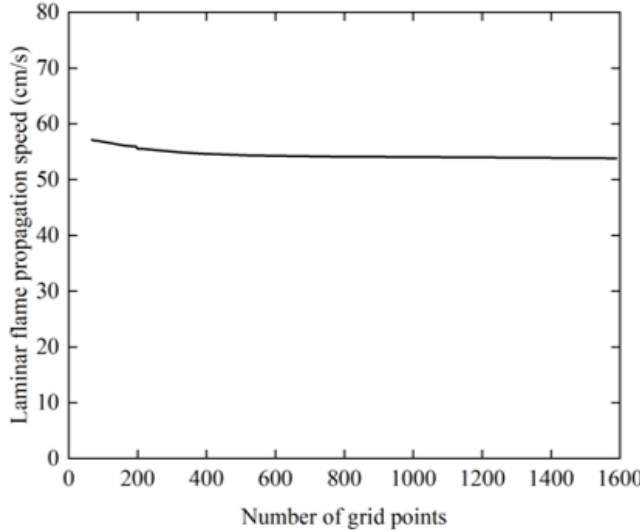


**Figure 1.** Variation of laminar flame propagation speed of iso-octane–air flames with the number of grid points

## 2.2 Data Processing Method

The LBV can be calculated via mass conservation as follows:

$$LBV = S_b^0 \cdot \rho_b / \rho_u = S_b^0 / \sigma \quad (1)$$

where,  $S_b^0$  is the unstretched laminar flame propagation speed,  $\rho_b$  and  $\rho_u$  are the densities of burned and unburned mixtures, respectively, and  $\sigma$  is the density ratio.

According to the cellular instability analysis theory [11, 12, 18], the instantaneous flame surface of a spherically expanding flame can be expressed as  $r = R_f(t)$ . When the flame front is disturbed, it can be expressed as:

$$r = R_f(t) [1 + A(t)S_n(\theta, \varphi)] \quad (2)$$

where,  $S_n$  denotes the spherical harmonic,  $n$  is the wave number,  $A$  is the disturbance amplitude, and  $\theta$  and  $\varphi$  are the polar angle and azimuth angle in the spherical coordinate system, respectively [19].

Flame stability analysis was conducted to reveal the effect of equivalence ratio and mixing ratio on the cellular instability of iso-octane/n-butanol–air flames, where the logarithmic growth rate of disturbance ( $A$ ) is used to identify the transition from stable to unstable status:

$$A(n, Pe) = d\ln A / d\ln Pe = \omega - \Omega / Pe \quad (3)$$

where,  $Pe$  is the Peclet number which is the dimensionless flame radius normalized by flame thickness,  $\omega$  and  $\Omega / Pe$  denote the contribution of hydrodynamic and diffusive-thermal instability, respectively.

The parameter  $\omega$  is expressed as:

$$\omega = \left[ -(b - a) + \sqrt{(b - a)^2 - 4ac} \right] / 2a \quad (4)$$

where, coefficients  $a$ ,  $b$  and  $c$  are determined by  $\sigma$  and  $n$ :

$$\begin{aligned} a &= (\sigma + 1)n + 1 \\ b &= 2n^2 + (4 + 5\sigma)n + 4 \\ c &= -[(\sigma - 1)/\sigma]n^3 + 2n^2 + \beta(\sigma + 1) - 1/\sigma n + 2 \end{aligned} \quad (5)$$

The detailed expression of  $\Omega$  is shown as:

$$\Omega = Q_1 + [Z(Le_{eff} - 1) / (\sigma - 1)]Q_2 + PrQ_3 \quad (6)$$

where,  $Q_1$ ,  $Q_2$  and  $Q_3$  are parameters representing the effects of thermal, molecular and viscous diffusion, respectively, which also depend on  $\sigma$  and  $n$ :

$$\begin{aligned} Q_1 &= (\gamma_1/\sigma\Delta) [n^4(\sigma+1) + \sigma n^3(2\omega+5) + n^2(\omega\sigma - 2\sigma^2 + \sigma - 1) + n\sigma(\sigma - 7 - 3\omega - \sigma\omega) \\ &\quad - 2\sigma(1+\omega)] + (\gamma_3/\sigma\Delta) [n(n^2-1)(n+2)(\sigma-1)] \\ Q_2 &= [\gamma_2(\sigma-1)/2\Delta] \times \{2n^4 + n^3(2\omega\sigma + 2\omega + 10\sigma - 3) + n^2[2\sigma\omega^2 + (5\sigma-1)\omega + 3\sigma - 2\sigma^2 - 2] \\ &\quad + n[\sigma\omega^2(1-4\sigma) - (14\sigma^2+1)\omega + 3 - 9\sigma - 8\sigma^2] - 2\sigma(\omega^2 + 4\omega + 3)\} \\ Q_3 &= [2n(n^2-1)(\sigma-1)/\sigma\Delta] \times [(n+2)(\lambda_b - \gamma_3) - 3(\lambda_b - 1)] \end{aligned} \quad (7)$$

where,  $\lambda_b$  indicates the thermal conductivity of the burned mixtures.  $\Delta$  and  $\gamma_3$  are calculated by:

$$\begin{aligned} \Delta &= 2a\omega + b - 2a \\ \gamma_3 &= \frac{\sigma}{\sigma-1} \int_1^\sigma \frac{\lambda(x)}{x} dx \end{aligned} \quad (8)$$

$Z$  is the Zeldovich number and  $Pr$  is the Prandtl number obtained respectively by the following formula:

$$\begin{aligned} Z &= E_a(T_b - T_u)/R^0 T_b^2 \\ Pr &= \mu C_p / \lambda \end{aligned} \quad (9)$$

where,  $E_a$  is the overall activation energy,  $T_b$  and  $T_u$  are the temperature of burned and unburned mixtures, respectively,  $\mu$  is the kinematic viscosity, and  $C_p$  is the heat capacity.

The effective Lewis number  $Le_{eff}$  is computed via:

$$Le_{eff} = 1 + \frac{(Le_E - 1) + (Le_D - 1) \cdot [1 + Z(\Phi - 1)]}{1 + [1 + Z(\Phi - 1)]} \quad (10)$$

where,  $Le$  is the Lewis number, with subscripts  $E$  and  $D$  denoting the excess reactant and deficient reactant, respectively, and  $\Phi$  is the ratio of the mass of excess-to-deficient reactants relative to their stoichiometric ratio.

The flame thickness  $\delta$  is acquired by:

$$\delta = \frac{T_b - T_u}{(dT/dx)_{max}} \quad (11)$$

where,  $(dT/dx)_{max}$  means the maximum temperature gradient.

### 3 Results and Discussion

#### 3.1 System Validation

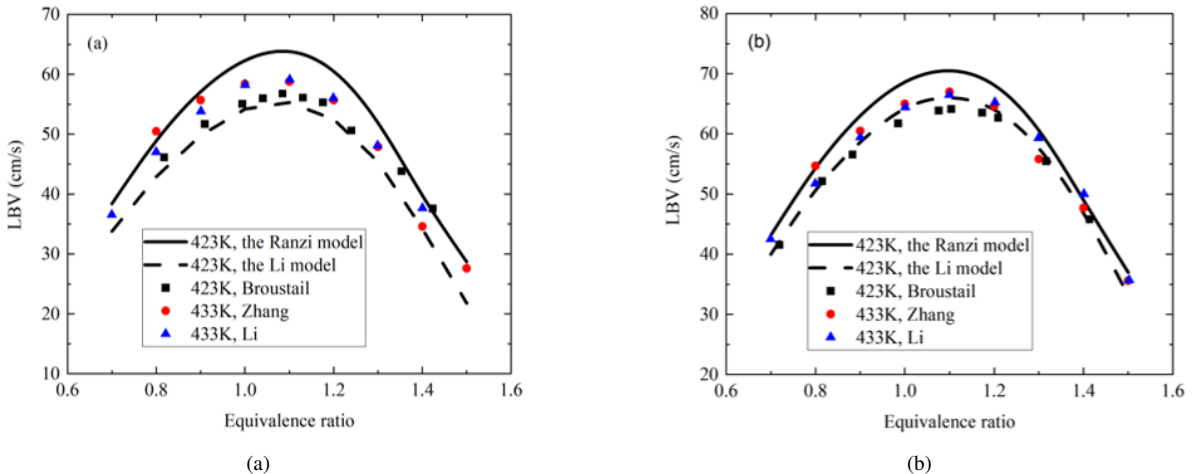


**Figure 2.** Comparison of laminar burning velocity (LBV) of: (a) iso-octane–air flames; (b) n-butanol–air flames in this study with literature data

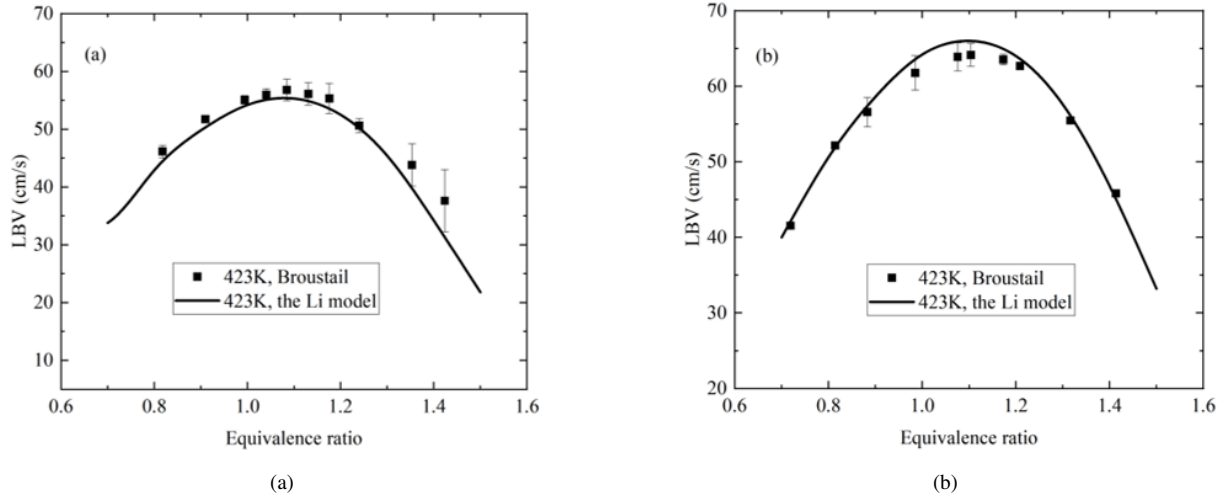


**Figure 3.** Comparison of LBV of: (a) iso-octane–air flames; (b) n-butanol–air flames by the Li Kinetic Model with experimental data

To verify the reliability of the numerical simulation and the data processing method, the simulated LBV of iso-octane–air flames and n-butanol–air flames at 423 K and 1 atm were compared with experimental data from previous research [17, 20, 21], as shown in Figure 2. It is evident that the LBV obtained by the Li Kinetic Model is reasonable in accordance with the experimental data, which validates the numerical simulation and the data processing method used in this study. While the Ranzi Kinetic Model overestimates LBV, especially for stoichiometric mixtures, it costs more time to complete the calculation due to more species and more reactions contained in this mechanism. As a result, the Li Kinetic Model was chosen for further simulation, and a detailed comparison of LBV using this model with experimental data by Broustail et al. [20] at 423 K is illustrated in Figure 3 with an error bar of residue, which shows acceptable agreement between the two, except for the iso-octane–air flame under highly fuel-rich conditions.

### 3.2 Flame Propagation

#### 3.2.1 Laminar burning velocity

The LBV of iso-octane/n-butanol–air flames at 423 K and 1 atm is plotted as a function of equivalence ratio in Figure 4. The mixing ratio  $\alpha$  is presented by the fraction of n-butanol in the blended fuel. It can be observed that the maximum values of the LBV appear at the equivalence ratio of 1.1 and decrease basically in both the rich and lean sides. Besides, the addition of n-butanol has a positive effect on LBV, especially near the stoichiometric condition. For the  $\varphi = 1.1$  condition, the LBV increases by 2.0%, 4.5%, 8.0% and 12.8% when 20%, 40%, 60% and 80% n-butanol are added in the fuel mixture, respectively.

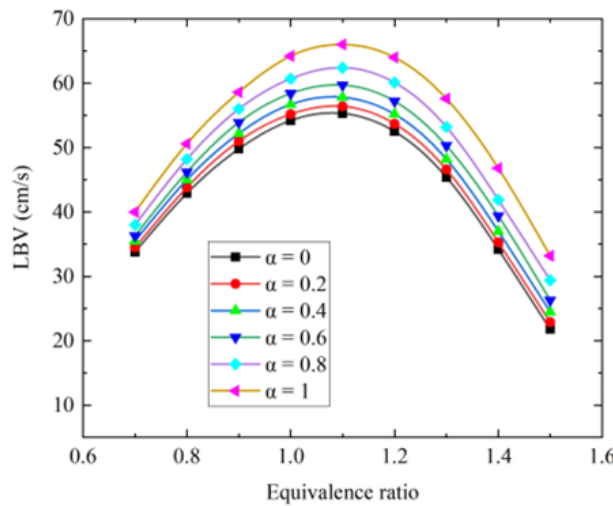


**Figure 4.** LBV of iso-octane/n-butanol–air flames at 423 K and 1 atm

### 3.2.2 Markstein length

As a dimensionless physical quantity that characterizes the sensitivity of flame propagation to local stretch, the  $L_b$  of burned mixtures is one of the important parameters in the study of fuel combustion characteristics. Based on previous research, a positive  $L_b$  indicates that the flame decelerates as the stretch rate increases, which tends to propagate in a relatively stable state, whereas a negative  $L_b$  means that the flame accelerates as the stretch rate increases, leading to relatively unstable propagation and distortion [22]. Both experimental and simulated investigations have been conducted to acquire the  $L_b$  of HC and its oxygen-containing components as well as its binary and ternary mixtures [23–25]. As depicted in Figure 5, the  $L_b$  of iso-octane/n-butanol–air flames reaches its minimum value at the equivalence ratio of 1.3, indicating the most unstable flame propagation at this point. It is evident that n-butanol addition promotes the flame instability of iso-octane/n-butanol–air flames since  $L_b$  decreases as the mixing ratio increases.

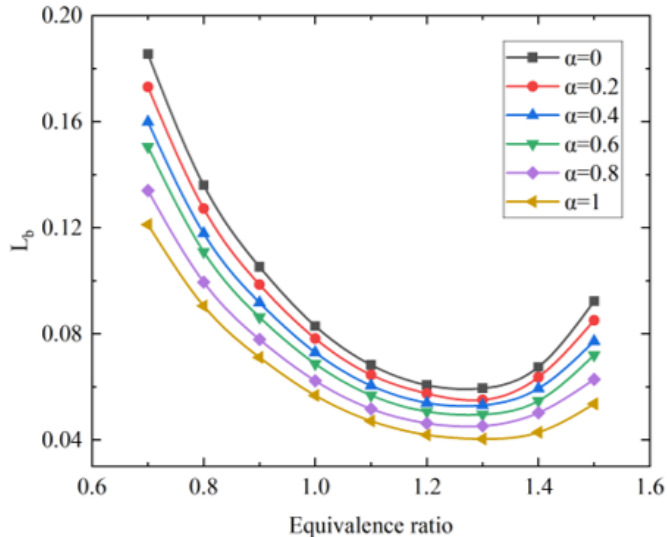


**Figure 5.** Markstein length ( $L_b$ ) of iso-octane/n-butanol–air flames at 423 K and 1 atm

### 3.3 Flame Instability

According to a previous study of Law [26], there are three types of cellular instability in spherical flames: buoyant instability, diffusive-thermal instability and hydrodynamic instability. As buoyant instability has been revealed to be remarkable only when the LBV is less than 10 cm/s [27], this type of instability was ignored because the lowest LBV in this study was 21.8 cm/s for iso-octane–air flames at the equivalence ratio of 1.5.

#### 3.3.1 Diffusive-thermal instability and hydrodynamic instability

Lewis number ( $L_e$ ), as a parameter indicating the competition between heat conduction and reactant diffusion, can be used to characterize the diffusive-thermal instability of a flame. Due to the different diffusivities of various components in the mixture, the initial planar flame is disturbed into an alternately concave-convex flame propagating toward the unburned side. For flames with a  $L_e$  greater than 1 ( $L_e > 1$ ), combustion intensifies at the concave parts and weakens at the convex parts, which tends to smooth out the wrinkles. Conversely, for flames with  $L_e < 1$ , the degree of wrinkling intensifies accordingly, leading to flame instability. Figure 6 illustrates the effective Lewis number ( $Le_{eff}$ ) of iso-octane/n-butanol–air flames. Obviously, the  $Le_{eff}$  decreases monotonically with the increase of equivalence ratio, suggesting that the flames of rich mixtures are more significantly affected by thermal-diffusive instability than those of lean mixtures. For the same equivalence ratio, the addition of n-butanol causes the flame to be more unstable with lower  $Le_{eff}$ .

Hydrodynamic instability is caused by the density step across the flame surface. It is prominently controlled by flame thickness ( $\delta$ ) and density ratio ( $\sigma$ ), and thinner  $\delta$  or higher  $\sigma$  indicates stronger hydrodynamic instability. Figure 7 depicts the simulated  $\delta$  and  $\sigma$  of iso-octane/n-butanol–air flames, both of which exhibit non-monotonic variation with equivalence ratio. The  $\delta$  first decreases and then increases as the equivalence ratio elevates, whereas an opposite trend is seen with regard to the  $\sigma$ . Therefore, the hydrodynamic instability of iso-octane/n-butanol–air flames first rises and then declines with the increase of equivalence ratio. On the other hand, the  $\delta$  decreases as the proportion of n-butanol in the mixture increases, promoting the hydrodynamic instability, whereas the  $\sigma$  keeps almost unchanged.

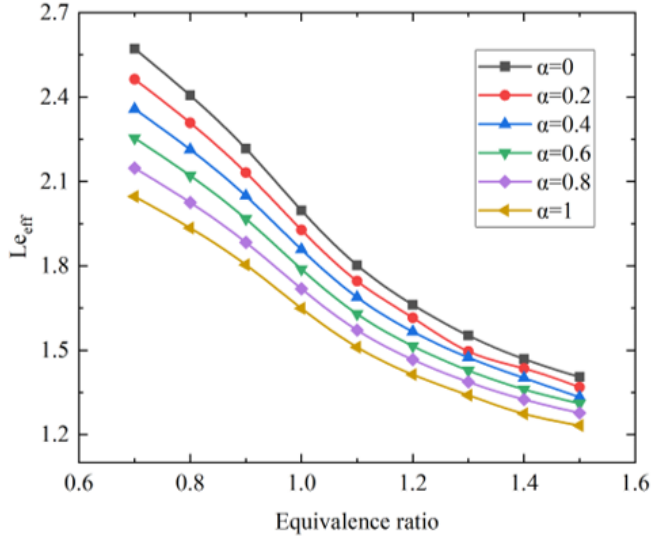


**Figure 6.** Effective Lewis number ( $Le_{eff}$ ) of iso-octane/n-butanol–air flames at 423 K and 1 atm

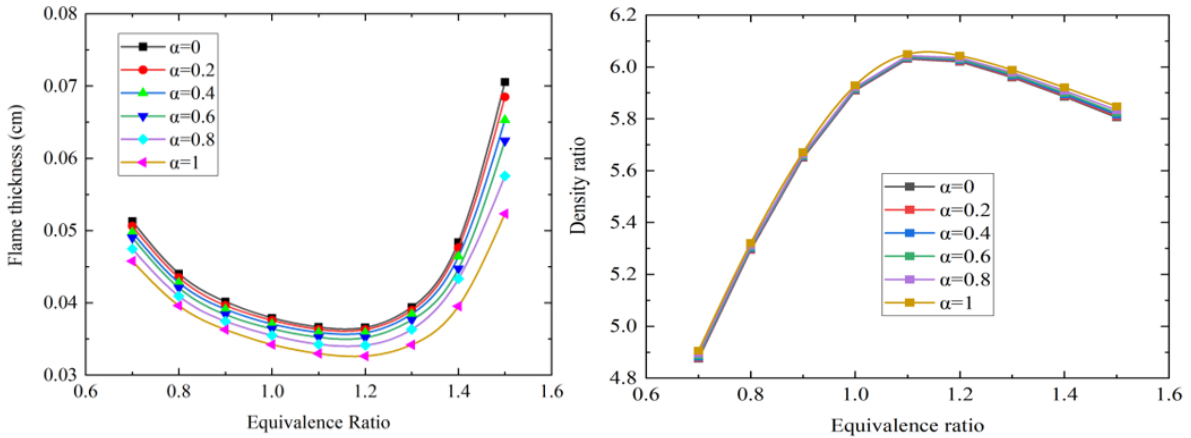


**Figure 7.** Flame thickness ( $\delta$ ) and density ratio ( $\sigma$ ) of iso-octane/n-butanol–air flames at 423 K and 1 atm

### 3.3.2 Critical Peclet number

Law et al. [13] proposed an asymptotic theory for the evolution of cellular structures on the flame surface, and the dimensionless  $Pe$  was defined as the characteristic parameter for the critical instability state. Bradley and Harper [18] conducted experimental studies on the cellularization process of spherically expanding flame surfaces. It was found that as the flame expands, a small number of cracks gradually form on the initially smooth flame surface, which gradually extend and split at high curvature locations to form new cracks when the flame size further increases, eventually evolving into a cellular structure that covers the entire front surface, and the flame propagation speed increases significantly accordingly. The critical  $Pe$  was defined in their study, based on the flame size when cracks initially appear. By setting the logarithmic growth rate of disturbance ( $A$ ) to 0, the dimensionless neutral stability curve of premixed iso-octane/n-butanol–air flames at 423 K and 1 atm was obtained, as shown in Figure 8. As shown in the figure, the plot is divided into two regions bounded by a curve, which is composed of two upper and lower branches, representing the effects of thermal diffusion and hydrodynamics, respectively. The region where  $A < 0$  represents a stable flame, while the region where  $A > 0$  indicates that the flame propagates in an unstable mode. The critical point ( $Pe, n_c$ ) where  $A$  transitions can be acquired from the vertex of the curve.

Figure 9 illustrates the calculated critical  $Pe$  of iso-octane/n-butanol–air flames at 423 K and 1 atm. It can be observed that the critical  $Pe$  decreases monotonously with increasing equivalence ratio, indicating that the fuel-rich mixtures tend to suffer cellular instability earlier than fuel-lean mixtures. Meanwhile, the critical  $Pe$  is also sensitive to the mixing ratio, and flame instability is promoted by the addition of n-butanol in the fuel mixture.

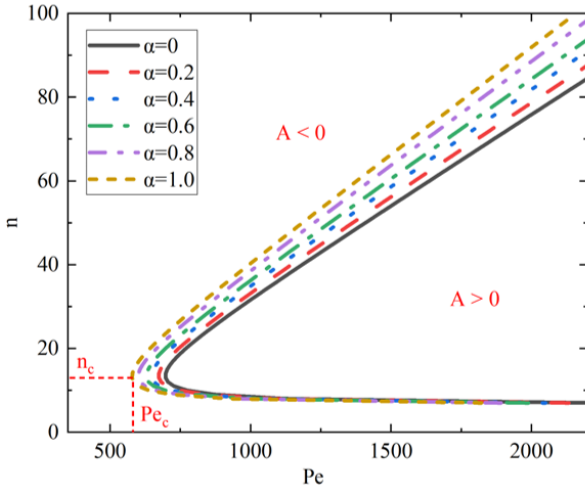


**Figure 8.** Neutral stability curve of stoichiometric iso-octane/n-butanol–air flames at 423 K and 1 atm

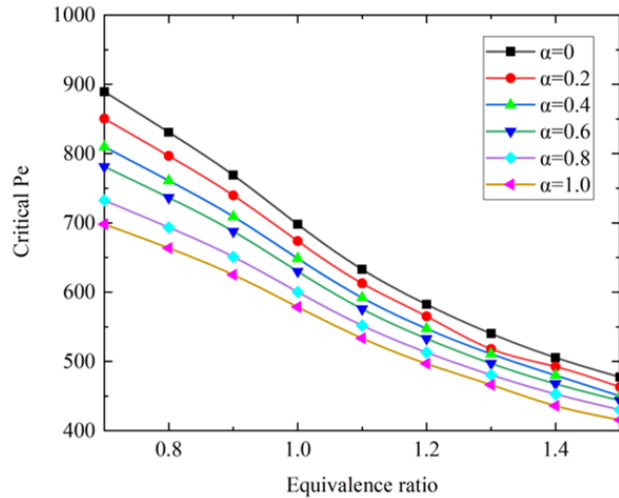


**Figure 9.** Critical Peclet number ( $P_e$ ) of iso-octane/n-butanol–air flames at 423 K and 1 atm

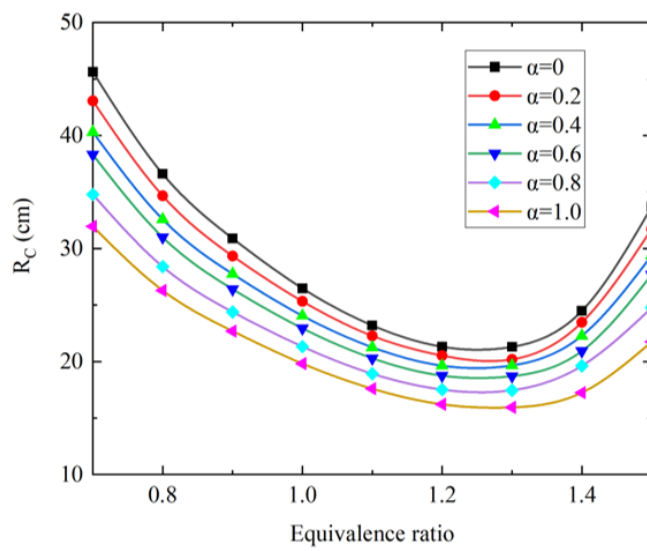


**Figure 10.** Critical flame radius ( $R_c$ ) of iso-octane/n-butanol–air flames at 423 K and 1 atm

### 3.3.3 Critical flame radius

The calculated critical flame radius ( $R_c$ ), used to measure the timing of the onset of cellular instability in spherical flames, can be obtained by the product of the critical  $Pe$  and  $\delta$ . Figure 10 depicts the  $R_c$  of iso-octane/n-butanol–air flames at 423 K and 1 atm. It is evident that the  $R_c$  changes non-monotonically with the increase of equivalence ratio and the minimum value appears approximately when  $\varphi = 1.3$ . This is caused by the non-monotonic change of  $\delta$ , as shown in Figure 7. Whereas the value of the  $R_c$  is decreased when the mixing ratio is increased, indicating that more n-butanol addition can promote the occurrence of cellular instability to a smaller radius.

## 4 Conclusions

The LBV and cellular instability of premixed iso-octane/n-butanol–air flames with various mixing ratios were investigated for a wide range of equivalence ratios (0.7–1.5) at an initial temperature of 423 K and ambient pressure. The main conclusions of this study are summarized as follows:

(a) With the addition of n-butanol, the LBV increases while the  $L_b$  decreases. The maximum value of LBV appears at the equivalence ratio of 1.1 and the minimum value of  $L_b$  appears at the equivalence ratio of 1.3 at a fixed mixing ratio.

(b) The diffusive-thermal instability enhances with increasing equivalence ratio, indicating that flame propagates in a more unstable state at the fuel-rich side, whereas the hydrodynamic instability first rises and then declines with the increase of equivalence ratio. Addition of n-butanol promotes both the diffusive-thermal instability and the hydrodynamic instability.

(c) The values of the critical  $Pe$  decrease monotonically with increasing equivalence ratio, but the  $R_c$  changes non-monotonically with the increase of equivalence ratio. The values of  $Pe$  and  $R_c$  decrease when more n-butanol is added to the fuel mixture.

(d) As a typical representative component of biomass fuels, n-butanol effectively improves the laminar flame speed, which is conducive to accelerating the combustion process and enhancing the power performance of engines. In contrast, the addition of n-butanol intensifies flame instability, and this is particularly prominent under fuel-rich conditions. Hence, more attention must be paid to combustion stability during practical operation to avoid incomplete combustion, reduced power output, or even engine failure caused by instability.

## Funding

This work is funded by Science Research Project of Hebei Education Department (Grant No.: QN2023208).

## Data Availability

The data used to support the research findings are available from the corresponding author upon request.

## Conflicts of Interest

The author declares no conflicts of interest.

## References

- [1] J. Lelieveld, A. Haines, R. Burnett, C. Tonne, K. Klingmüller, T. Münzel, and A. Pozzer, “Air pollution deaths attributable to fossil fuels: Observational and modelling study,” *BMJ*, vol. 383, p. e077784, 2023. <https://doi.org/10.1136/bmj-2023-077784>
- [2] B. H. Kreps, “The rising costs of fossil-fuel extraction: An energy crisis that will not go away,” *Am. J. Econ. Sociol.*, vol. 79, no. 3, pp. 695–717, 2020. <https://doi.org/10.1111/ajes.12336>
- [3] H. Joshi, J. Toler, B. R. Moser, and T. Walker, “Biodiesel from canola oil using a 1: 1 molar mixture of methanol and ethanol,” *Eur. J. Lipid Sci. Technol.*, vol. 111, no. 5, pp. 464–473, 2009. <https://doi.org/10.1002/ejlt.200800071>
- [4] M. Obergruber, V. Hönig, J. Jenčík, J. Hájek, D. Schlehöfer, and T. Herink, “Lignocellulosic bioethanol and biobutanol as a biocomponent for diesel fuel,” *Materials*, vol. 14, no. 19, p. 5597, 2021. <https://doi.org/10.3390/ma14195597>
- [5] Ö. L. Gülder, “Burning velocities of ethanol-isoctane blends,” *Combust. Flame*, vol. 56, no. 3, pp. 261–268, 1984. [https://doi.org/10.1016/0010-2180\(84\)90060-9](https://doi.org/10.1016/0010-2180(84)90060-9)
- [6] J. P. J. Van Lipzig, E. J. K. Nilsson, L. P. De Goey, and A. A. Konnov, “Laminar burning velocities of n-heptane, iso-octane, ethanol and their binary and tertiary mixtures,” *Fuel*, vol. 90, no. 8, pp. 2773–2781, 2011. <https://doi.org/10.1016/j.fuel.2011.04.029>
- [7] P. Dirrenberger, P. A. Glaude, R. Bounaceur, H. Le Gall, A. P. Da Cruz, A. A. Konnov, and F. Battin-Leclerc, “Laminar burning velocity of gasolines with addition of ethanol,” *Fuel*, vol. 115, pp. 162–169, 2014. <https://doi.org/10.1016/j.fuel.2013.07.015>

- [8] O. A. Manna, M. S. Mansour, W. L. Roberts, and S. H. Chung, "Laminar burning velocities of fuels for advanced combustion engines (FACE) gasoline and gasoline surrogates with and without ethanol blending associated with octane rating," *Combust. Sci. Technol.*, vol. 188, no. 4–5, pp. 692–706, 2016. <https://doi.org/10.1080/00102202.2016.1138812>
- [9] Z. Meng, K. Liang, and J. Fang, "Laminar burning velocities of iso-octane, toluene, 1-hexene, ethanol and their quaternary blends at elevated temperatures and pressures," *Fuel*, vol. 237, pp. 630–636, 2019. <https://doi.org/10.1016/j.fuel.2018.10.072>
- [10] S. Yang, A. Saha, F. Wu, and C. K. Law, "Morphology and self-acceleration of expanding laminar flames with flame-front cellular instabilities," *Combust. Flame*, vol. 171, pp. 112–118, 2016. <https://doi.org/10.1016/j.combustflame.2016.05.017>
- [11] J. K. Bechtold and M. Matalon, "Hydrodynamic and diffusion effects on the stability of spherically expanding flames," *Combust. Flame*, vol. 67, no. 1, pp. 77–90, 1987. [https://doi.org/10.1016/0010-2180\(87\)90015-0](https://doi.org/10.1016/0010-2180(87)90015-0)
- [12] R. Addabbo, J. K. Bechtold, and M. Matalon, "Wrinkling of spherically expanding flames," *Proc. Combust. Inst.*, vol. 29, no. 2, pp. 1527–1535, 2002. [https://doi.org/10.1016/S1540-7489\(02\)80187-0](https://doi.org/10.1016/S1540-7489(02)80187-0)
- [13] C. K. Law, G. Jomaas, and J. K. Bechtold, "Cellular instabilities of expanding hydrogen/propane spherical flames at elevated pressures: Theory and experiment," *Proc. Combust. Inst.*, vol. 30, no. 1, pp. 159–167, 2005. <https://doi.org/10.1016/j.proci.2004.08.266>
- [14] G. Wang, Y. Li, L. Li, and F. Qi, "Experimental and theoretical investigation on cellular instability of methanol/air flames," *Fuel*, vol. 225, pp. 95–103, 2018. <https://doi.org/10.1016/j.fuel.2018.03.160>
- [15] F. Oppong, C. Xu, L. Zhongyang, X. Li, W. Zhou, and C. Wang, "Cellularization of 2-methylfuran expanding spherical flame," *Combust. Flame*, vol. 206, pp. 379–389, 2019. <https://doi.org/10.1016/j.combustflame.2019.05.023>
- [16] E. L. I. S. E. O. Ranzi, A. Frassoldati, R. Grana, A. Cuoci, T. Faravelli, A. P. Kelley, and C. K. Law, "Hierarchical and comparative kinetic modeling of laminar flame speeds of hydrocarbon and oxygenated fuels," *Prog. Energy Combust. Sci.*, vol. 38, no. 4, pp. 468–501, 2012. <https://doi.org/10.1016/j.pecs.2012.03.004>
- [17] X. Li, E. Hu, X. Meng, X. Lu, and Z. Huang, "High-temperature oxidation kinetics of iso-octane/n-butanol blends-air mixture," *Energy*, vol. 133, pp. 443–454, 2017. <https://doi.org/10.1016/j.energy.2017.05.111>
- [18] D. Bradley and C. M. Harper, "The development of instabilities in laminar explosion flames," *Combust. Flame*, vol. 99, no. 3–4, pp. 562–572, 1994. [https://doi.org/10.1016/0010-2180\(94\)90049-3](https://doi.org/10.1016/0010-2180(94)90049-3)
- [19] M. Matalon, "Intrinsic flame instabilities in premixed and nonpremixed combustion," *Annu. Rev. Fluid Mech.*, vol. 39, no. 1, pp. 163–191, 2007. <https://doi.org/10.1146/annurev.fluid.38.050304.092153>
- [20] G. Broustail, F. Halter, P. Seers, G. Moréac, and C. Mounaïm-Rousselle, "Experimental determination of laminar burning velocity for butanol/iso-octane and ethanol/iso-octane blends for different initial pressures," *Fuel*, vol. 106, pp. 310–317, 2013. <https://doi.org/10.1016/j.fuel.2012.10.066>
- [21] X. Zhang, C. Tang, H. Yu, Q. Li, J. Gong, and Z. Huang, "Laminar flame characteristics of iso-octane/n-butanol blend-air mixtures at elevated temperatures," *Energ. Fuels*, vol. 27, no. 4, pp. 2327–2335, 2013. <https://doi.org/10.1021/ef4001743>
- [22] D. Bradley, R. A. Hicks, M. Lawes, C. G. Sheppard, and R. Woolley, "The measurement of laminar burning velocities and markstein numbers for iso-octane-air and iso-octane-n-heptane-air mixtures at elevated temperatures and pressures in an explosion bomb," *Combust. Flame*, vol. 115, no. 1–2, pp. 126–144, 1998. [https://doi.org/10.1016/S0010-2180\(97\)00349-0](https://doi.org/10.1016/S0010-2180(97)00349-0)
- [23] M. Tippa, M. Akash, S. Subbiah, and C. Prathap, "A comprehensive study on laminar burning velocity and flame stability of oxy-producer gas mixtures. Part-2: Laminar burning velocity and markstein length analysis," *Fuel*, vol. 292, p. 119982, 2021. <https://doi.org/10.1016/j.fuel.2020.119982>
- [24] V. Shankar, X. H. Fang, N. Hinton, M. Davy, and F. C. P. Leach, "Effect of ethanol addition on the laminar burning velocities of gasoline surrogates," *Fuel*, vol. 327, p. 125186, 2022. <https://doi.org/10.1016/j.fuel.2022.125186>
- [25] A. K. Marwaan, J. Yang, A. S. Tomlin, H. M. Thompson, G. de Boer, K. Liu, and M. E. Morsy, "Laminar burning velocities and Markstein numbers for pure hydrogen and methane/hydrogen/air mixtures at elevated pressures," *Fuel*, vol. 354, p. 129331, 2023. <https://doi.org/10.1016/j.fuel.2023.129331>
- [26] C. K. Law, *Combustion Physics*. Cambridge University Press, 2006.
- [27] G. Li, M. Zhou, Z. Zhang, J. Liang, and H. Ding, "Experimental and kinetic studies of the effect of CO<sub>2</sub> dilution on laminar premixed n-heptane/air flames," *Fuel*, vol. 227, pp. 355–366, 2018. <https://doi.org/10.1016/j.fuel.2018.04.116>